Effect of Na+-channel blockade on the three-dimensional substrate of atrial fibrillation in a model of endo-epicardial dissociation and transmural conduction

Ali Gharaviri, Sander Verheule, Jens Eckstein, Mark Potse, Rolf Krause, Angelo Auricchio, Nico H.L. Kuijpers, Ulrich Schotten

Effect of Na^+-channel blockade on the three-dimensional substrate of atrial fibrillation in a model of endo-epicardial dissociation and transmural conduction

Ali Gharaviri, PhD,[1,2], Sander Verheule, PhD,[1] Jens Eckstein, MD, PhD,[1,3] Mark Potse, PhD,[4,5,6] Rolf Krause, PhD[2], Angelo Auricchio, MD, PhD,[2,7] Nico H.L. Kuijpers, PhD,[8] Ulrich Schotten, MD, PhD[1]

1: Dept. of Physiology, Maastricht University, Maastricht, The Netherlands.
2: Center for Computational Medicine in Cardiology, Institute of Computational Science, Università della Svizzera italiana, Lugano, Switzerland.
3: University Hospital Basel, Dept. of Internal Medicine, Basel, Switzerland.
4: Carmen team, Inria Bordeaux Sud-Ouest, Talence, France.
5: Université de Bordeaux, IMB, UMR 5251, F-33400 Talence, France.
6: IHU Liryc, Electrophysiology and Heart Modeling Institute, foundation Bordeaux Université, Bordeaux, France.
7: Fondazione Cardiocentro Ticino, Lugano, Switzerland.
8: Dept. of Biomedical Engineering, Maastricht University, Maastricht, The Netherlands.

Institution where work was done: Dept. of Physiology, Maastricht University, Maastricht, The Netherlands.

Abstract

Introduction:

Atrial fibrillation (AF) is a progressive arrhythmia characterized by structural alterations that increase its stability. Both clinical and experimental studies showed a concomitant loss of antiarrhythmic drug efficacy in later stages of AF. The mechanisms underlying this loss of efficacy are not well understood. We hypothesized that structural remodeling may explain this reduced efficacy by making the substrate more three-dimensional. To investigate this, we simulated the effect of sodium channel block on AF in a model of progressive transmural uncoupling.

Methods:

In a computer model consisting of 2 cross-connected atrial layers, with realistic atrial membrane behavior, structural remodeling was simulated by reducing the number of connections between the layers. 100% endo-epicardial connectivity represented a healthy atrium. At various degrees of structural remodeling, we assessed the effect of 60% sodium channel block on AF stability, endo-epicardial electrical activity dissociation (EED), and fibrillatory conduction pattern complexity quantified by number of waves, phase singularities (PSs), and transmural conduction ("breakthrough", BT).

Results:

Sodium channel block terminated AF in non-remodeled but not in remodeled atria. The temporal excitable gap and atrial fibrillation cycle length increased at all degrees of remodeling compared to control. Despite an increase of EED and excitable gap, sodium channel block decreased the incidence of BT because of transmural conduction block. Sodium channel block decreased the number of waves and phase singularities (PSs) in normal atrium but not in structurally remodeled atrium.

Conclusions:

This simple atrial model explains the loss of efficacy of sodium channel block in terminating AF in the presence of severe structural remodeling as has been observed experimentally and clinically. AF termination in atria with moderate structural remodeling in the presence of sodium channel block is caused by reduction of AF complexity. With more severe structural remodeling, sodium channel block fails to promote synchronization of the two layers of the model.

Condensed Abstract:

Structural remodeling during atrial fibrillation (AF) adds more three-dimensional character to AF conduction patterns. Based on previous experimental studies, this could explain the loss of sodium channel blocker efficacy in patients in later stages of AF. To test this hypothesis, we used a previously developed proof-of-principle model, which was able to simulate this three-dimensional characteristic of AF conduction.

What is new:

- Using this model, we could simulate three-dimensional characteristics of AF conduction patterns, which occur in the later stages of AF, and investigate whether this could be a possible mechanisms underlying sodium channel blocker efficacy loss in patients in later stages of AF.
- Decrease in the degree of coupling between endocardium and epicardium caused a significant decrease in the efficacy of sodium channel blocker in AF termination.
- Increase in the degree of endo-epicardial electrical activity dissociation and BTs was the strongest determinant of AF persistence in all simulations in the presence of sodium channel blockers.

Abbreviations:

AF = atrial fibrillation; **PS** = phase singularities; **BT** = breakthrough; **BTR** = breakthrough rates; **AFCL** = atrial fibrillation cycle length; **EG** = excitable gap.

1. Introduction

Atrial fibrillation (AF) is known to induce significant electrophysiological alterations in atrial myocytes and causes significant structural changes (structural remodelling). Several studies have demonstrated that structural remodeling, including fibrosis, is associated with a decrease in the size of fibrillatory waves, an increase in the electrical activity dissociation between the epicardial layer and the endocardial bundle network, and an increase in the incidence of transmural conduction ("breakthroughs").(1-3)

Numerous therapeutic strategies, ranging from pharmaceutical interventions to ablation, have been used in AF treatment. Anti-arrhythmic drugs have been an important part of AF therapy for many years.(4-8) Among all anti-arrhythmic drugs, sodium (Na^+)-channel blockers have a long history in AF treatment.(5-10) Recent studies witness an increased interest in Na^+-channel blockers such as flecainide for AF therapy. (5,9-11) Although several studies have been performed on Na^+-channel blockers it is not clear how these agents facilitate cardioversion of AF and why they are less effective in advanced stages of AF, as clinical studies have reported.(5,8,10) Three possible mechanisms of cardioversion have been proposed including (1) enlargement of PS tips, (2) decreased anchoring of rotors to functional obstacles, and (3) reduction in number of waves, due to an increase in the excitable gap (EG).(12) While all simulation studies reported a high success rate in AF termination by the application of Na^+-channel blockers, several experimental studies have revealed a reduction in termination rates after administration of Na^+-channel blockers in both animal models and patients in later stages of AF.(5,6,8-10,13) Recently one possible mechanism for this efficacy loss has been proposed by Eckstein et al.(13) This study suggested that the three-dimensional substrate of AF conduction, which occurs in the later stages of AF and due to structural remodeling, could have an important effect on sodium channel block efficacy of AF termination. (13) In this work it was demonstrated

that flecainide reduced the incidence of BTs and endo-epicardial electrical dissociation significantly. (13) This aspect, three-dimensional substrate of AF, is missing in all simulation studies performed so far on the effect of sodium channel blocker on AF termination. All those simulations were performed in either a two-dimensional model or two-dimensional sheets of atrial myocytes folded into a 3D shape of human atria. Therefore, in the present study we used a previously developed dual layer model (14-16) which enabled us to study the effect of three-dimensional substrate on Na^+-channel blocker efficacy.

In the present study, we investigated why a Na^+-channel blocker is effective in early stages of AF but gradually loses its efficacy in the later stages of AF or, more precisely, with progressive structural remodeling. We hypothesized that the possible explanation for this loss is that structurally remodeled atria represent a higher degree of 3-dimensionality in the AF substrate. We addressed this hypothesis by assessing the effect of Na^+-channel blockade on endo-epicardial electrical activity dissociation, transmural conduction and AF stability at different degrees of structural remodeling.

2. Methods

2.1. Model

To investigate the effect of Na^+-channel blockade on AF stability, endo-epicardial dyssynchrony, and breakthrough events during AF, we used a dual-layer computer model (figure 1A).(14) Human atrial electrophysiology was modeled with a mono-domain reaction-diffusion model comprising two layers with a size of 4cm × 4cm. Each of the layers was composed of 400 × 400 segments with a size of 0.01cm × 0.01cm. Ionic currents and calcium handling for each segment was described by the Courtemanche-Ramirez-Nattel model.(17) The tissue had an isotropic conductivity of 0.5 mS/cm. Total ionic membrane current was given by:

$$I_{ion} = I_{Na} + I_{K1} + I_{to} + I_{Kur} + I_{Kr} + I_{Ks} + I_{Ca,L} + I_{p,Ca} + I_{NaK} + I_{NaCa} + I_{b,Na} + I_{b,Ca} \quad (1)$$

where I_{Na} is fast inward Na^+ current, I_{K1} is inward rectifier K^+ current, I_{to} transient outward K^+ current, I_{kur} is ultrarapid delayed rectifier K^+ current, I_{kr} is rapid delayed rectifier current, I_{Ks} is slow delayed rectifier K^+ current, $I_{Ca,L}$ is L-type Ca^{2+} current, $I_{p,Ca}$ is Ca^{2+} pump current, I_{NaK} is Na^+-K^+ pump current, I_{NaCa} is Na^+/Ca^{2+} exchanger current, and $I_{b,Na}$ and $I_{b,Ca}$ are background Na^+ and Ca^{2+} currents. To incorporate changes in ionic currents that have been observed in AF, conductivities for I_{to}, $I_{Ca,L}$, and I_{K1} were set at 40%, 35%, and 200% of the default values, respectively.(14,18,19)

Electrical coupling between the two layers was implemented by adding an Ohmic conductor between opposing segments at so-called connection points. Each connection point was a circle with a radius of 0.1 cm.

2.2. Simulation protocol

To investigate the effect of Na^+-channel blockers on endo-epicardial electrical activity dissociation and transmural conduction at different stages of structural remodeling, the following simulation protocol was applied (see figure 1C):

1. In one layer, a spiral wave was initiated using an S1-S2 protocol, while the other layer was quiescent, as described in a previous study.(14) The simulation was continued for 1 second in order to achieve a stable spiral wave.
2. One second after the start of the simulation, 6 connection points were added at randomly chosen sites, with the constraint that two connection points were at least 0.15 cm apart. To exclude possible bias resulting from a particular geometry of connection points, 8 different geometries with 6 randomly chosen sites were created. For each of the 8 geometries, the simulation of step 1 was continued for 6 more seconds. This resulted in 8 different simulations that were used as a starting point of the next stages of the simulation.
3. The 8 simulations from step 2 were used and continued for another 6 seconds, either without changing the connection points or after adding more randomly chosen connection points (at least 0.15cm apart), so that the total number of connections was 6, 12, 24, 48 or 96. In addition, each simulation from step 2 was continued as well with 100% connectivity, which means that all opposing segments in the two layers were connected to one another.
4. All simulations at step 3 were simulated twice, once with the normal sodium conductance (control) and once with 60% sodium channel conductance block. As described above,

steps 2 and 3 were performed 8 times such that in total 48 simulation runs were performed in step 3.

In our model, 6 and 12 connections represented severely remodeled atria; 24 and 48 connections represented moderately remodeled atria, and 96 connections and 100% connectivity represented a healthy atrium.

2.3. Analysis

In all 48 simulations of step 3 the following parameters were analyzed as described previously(14,19):

- Number of phase singularities (PSs)
- Number of fibrillation waves
- Atrial fibrillation cycle length (AFCL)
- Temporal excitable gap (EG)
- Degree of endo-epicardial dyssynchrony
- Breakthrough rates (BTRs)
- AF stability

3. RESULTS

Figure 2 shows representative examples of AF in control and in the presence of Na^+-channel block for two different degrees of endo-epicardial connectivity (96 and 12 connections).
In 96 connections simulations - representing a healthy atrium - a large number of BTs occurred immediately after the additional connections were introduced, leading to effective synchronization of the two layers. Complete synchronization of the two layers on average took approximately 250ms. After synchronization, no BTs were observed, and the AF episode quickly terminated (see Figure 2). In contrast to 96 connections, in simulations with 12 connections BTs occurred throughout the simulation. However, none of those BTs could synchronize two layers.

3.1. AF stability

AF stability in different degrees of connectivity, with or without Na^+-channel block, is illustrated in the Kaplan-Meier curves in figure 3. As shown in this figure, in simulations with a high number of connections (96 connections and 100% connectivity), Na^+-channel block accelerated AF termination. Upon a progressive reduction in the connectivity between the two layers (48 and 24 connections) Na^+-channel block gradually lost its efficacy, and AF persistence became comparable with the control simulations. After a stronger reduction (6 and 12 connections) Na^+-channel block was not only able to facilitate AF termination but also made AF more stable compared to control simulations.

3.2. Effect of sodium channel blockade on fibrillation patterns

As described above, Na^+-channel block only decreased AF persistence in simulations with 96 connections and 100% connectivity. To understand this failure of AF termination in simulations

with a smaller number of connections, we tried to further assess the mechanisms causing AF termination by computing several electrophysiological parameters in all groups of simulations with or without Na^+-channel block (figure 4). As expected and reported in the previous studies(4,20), presence of Na^+-channel block increased the AF cycle length (AFCL) and the excitable gap (EG) in all groups of connectivity (figure 4A and B). The number of waves in both groups was similar, except at high degrees of connectivity, where Na^+-channel block decreased the number of waves (figure 4C). Similarly, Na^+-channel block decreased the number of PSs only for 96 connections and 100% connectivity (figure 4D). Dyssynchrony was not, or subtly, affected by Na^+-channel block, and the BT rate showed a non-significant trend towards a decrease in the presence of Na^+-channel block (figure 4E and F).

To further uncover the reasons underlying this efficacy loss, we divided the simulations in two groups, 3D and 2D. The 3D group contained simulations with 6 and 12 connections, and represented severely remodeled atrium. The 2D group contained 96 connections and 100% connectivity simulations, and represented healthy atrium. As expected and mentioned above, in the 3D group we observed a pronounced loss of efficacy of sodium channel blockade, while in the 2D group blocking Na^+-channel effectively terminated AF (see figure 5).

In both groups the presence of Na^+-channel block also significantly increased both the AFCL and EG compared to the control (see figure 6A and 6B). AF pattern complexity, quantified as the number of waves and PSs, in the 2D group was significantly lower in the presence of Na^+-channel blocker compared to control. Interestingly, the Na^+-channel blocker was unable to decrease AF pattern complexity in the simulations in the 3D group (see figure 6C and D). BTs, which are a reflection of 3-dimensional substrate of AF, were significantly reduced in the 3D group. This reduction in the number of BTs occurred, while the degree of endo-epicardial

dyssynchrony, which was the main cause of BT occurrences, remained unaltered in the presence of Na^+-channel block. The main argument, which can describe this phenomenon, is a pronounced increase in the number of unsuccessful BTs in all simulations regardless of the number of connections (figure 7).

4. Discussion

Although the effects of Na^+-channel blockade on AF have been studied extensively, the mechanism of AF termination by Na^+-channel block and the reason for the loss of its efficacy in structurally remodeled atria are poorly understood. These mechanisms are likely multifactorial, involving depression of excitability and impaired impulse propagation resulting in progressive merging of fibrillation waves in the presence of wide EG or enhanced meandering of rotors leading to collision of wave fronts with anatomical boundaries. (12,21-23)

Although simulation studies investigated several mechanisms underlying AF termination in the presence of Na^+-channel block, the question regarding the loss of efficacy of Na^+-channel block in later stages of AF is still unanswered. In a goat model of AF, it was demonstrated by Eijsbouts et al. that this loss of efficacy was not due to a loss of AFCL or temporal EG prolongation in the presence of the drug.(20) The study by Eckstein et al. suggests that the loss of AF termination rather could be due to the increasingly 3-dimensional conduction pattern of AF in later stages of remodeling.

4.1. Parameters determining AF stability

In the present study, we showed the efficacy loss of Na^+-channel blocker in AF termination in different stages of structural remodeling. In all simulations with no structural remodeling (96 connections and 100% connectivity) AF episodes terminated much faster in the presence of Na^+-channel blocker. However, in all simulations with severe structural remodeling (6 or 12 connections), Na^+-channel blocker was unable to terminate AF. Interestingly, we did not observe significant differences in AF termination rate between control and Na^+-channel block simulations with severe (6 and 12 connections) and moderate (24 and 48 connections) structural remodeling. AF termination rate was significantly different in 96 connections and 100%

connectivity simulations in the presence of Na^+-channel blocker compared to the control simulations. As illustrated in figures 4 and 6, AFCL and EG were increased in the presence of Na^+-channel blockade. These findings agreed with findings reported in previous studies.(12,24) Since this increase was present at all different numbers of connections and in both 2D and 3D groups, it cannot explain the loss of efficacy with structural remodeling in our model. The presence of Na^+-channel blocker decreased AF complexity, quantified as the number of waves and phase singularities, in the 2D group simulations, in which two layers were well coupled and degrees of dyssynchrony were low. Therefore, fibrillation waves could not find opportunities to propagate from one layer to the other. However, Na^+-channel blocker was unable to perform the same in the 3D group simulations. In this group the degree of dyssynchrony was higher due to a lower number of connections between two layers, and fibrillation waves could find more opportunities to propagate from one layer to the other. This inability of Na^+-channel block to reduce AF complexity in simulations of severe remodeling, which has a more 3-dimensional character, could be an explanation for the Na-channel blocker efficacy loss at the later stage of AF.

4.2. The effect of Na-channel blocker on dyssynchrony and BTs

In the goat atria, Eckstein et al showed a decrease in both endo-epicardial dissociation and BTs in the presence of flecainide.(13) In our model, we observed only a slight, insignificant increase in dyssynchrony as a result of Na^+-channel blockade, regardless of the degree of connectivity. At first glance, a similar degree of dyssynchrony in combination with an increase in EG should increase the number of opportunities for BTs to occur. However, we observed a decrease in BT incidence (see figure 4F). To investigate possible mechanisms for this reduction, we analyzed the number of unsuccessful BTs (figure 7B). Unsuccessful BT was defined as a BT that did not

conduct transmurally despite the presence of local endo-epicardial electrical dyssynchrony. A pronounced increase in the number of unsuccessful BTs as a result of Na^+-channel block was observed in all sets of connections (figure 7C). This transmural conduction block due to reduced excitability or a sink/source mismatch could explain the surprisingly low number of breakthroughs in the presence of Na^+-channel block (given the increase in excitable gap). However, the decline of the breakthrough rate in the presence of Na^+-channel block was obviously not strong enough to allow for sufficient reduction of AF complexity and AF termination.

4.3. Study Limitations

Our dual-layer model should be considered as a proof-of-principle model. This model does not reflect 3D geometry and complex structure of the atrium, fiber orientation arrangement, heterogeneity in ionic membrane currents, and variability in atrial wall thickness. According to this, the effect of myocardial thickness could not be addressed. In this study a simple pore-block model (a fixed percentage decrease in maximum Na^+ -channel conductance) was used to simulate Na^+-channel blockade. A more detailed exploration of the impact of state-dependent I_{Na} block as occurs for all clinically used class I drugs, with the application of a mathematical formulation of such action, would be of great interest but is beyond the scope of the present study. However, the work in this study does demonstrate for the first time that pure reduction of Na^+ current fails to terminate AF in the presence of severe structural remodeling leading to a three-dimensional substrate for AF.

We also did not consider ectopic focal discharges as a mechanism contributing to AF maintenance in this study. Despite these limitations, we have shown that our model is well suited

to investigate the effect of Na-channel blockers on endo-epicardial dissociation, breakthroughs and AF stability.

4.4. Conclusion

Using a simple bilayer model we have shown that severe structural remodeling, resulting in a small number of connections between the subendocardial and subepicardial layers of the atria, can prevent termination of AF by Na^+-channel block.

References

1. Verheule S, Tuyls E, van Hunnik A, Kuiper M, Schotten U, Allessie M. Fibrillatory conduction in the atrial free walls of goats in persistent and permanent atrial fibrillation. Circulation Arrhythmia and electrophysiology 2010;3:590-9.
2. de Groot NM, Houben RP, Smeets JL et al. Electropathological substrate of longstanding persistent atrial fibrillation in patients with structural heart disease: epicardial breakthrough. Circulation 2010;122:1674-82.
3. Allessie MA, de Groot NM, Houben RP et al. Electropathological substrate of long-standing persistent atrial fibrillation in patients with structural heart disease: longitudinal dissociation. Circulation Arrhythmia and electrophysiology 2010;3:606-15.
4. Comtois P, Sakabe M, Vigmond EJ et al. Mechanisms of atrial fibrillation termination by rapidly unbinding Na+ channel blockers: insights from mathematical models and experimental correlates. American journal of physiology Heart and circulatory physiology 2008;295:H1489-504.
5. Tieleman RG, Van Gelder IC, Bosker HA et al. Does flecainide regain its antiarrhythmic activity after electrical cardioversion of persistent atrial fibrillation? Heart Rhythm 2005;2:223-30.
6. Goy JJ, Grbic M, Hurni M et al. Conversion of supraventricular arrhythmias to sinus rhythm using flecainide. Eur Heart J 1985;6:518-24.
7. Goy JJ, Kaufmann U, Kappenberger L, Sigwart U. Restoration of sinus rhythm with flecainide in patients with atrial fibrillation. Am J Cardiol 1988;62:38D-40D.
8. Goy JJ, Maendly R, Grbic M, Finci L, Sigwart U. Cardioversion with flecainide in patients with atrial fibrillation of recent onset. Eur J Clin Pharmacol 1985;27:737-8.
9. Crijns HJ, van Wijk LM, van Gilst WH, Kingma JH, van Gelder IC, Lie KI. Acute conversion of atrial fibrillation to sinus rhythm: clinical efficacy of flecainide acetate. Comparison of two regimens. Eur Heart J 1988;9:634-8.
10. Aliot E, Capucci A, Crijns HJ, Goette A, Tamargo J. Twenty-five years in the making: flecainide is safe and effective for the management of atrial fibrillation. Europace 2011;13:161-73.
11. Nattel S, Carlsson L. Innovative approaches to anti-arrhythmic drug therapy. Nature reviews Drug discovery 2006;5:1034-49.
12. Kneller J, Kalifa J, Zou R et al. Mechanisms of atrial fibrillation termination by pure sodium channel blockade in an ionically-realistic mathematical model. Circulation research 2005;96:e35-47.
13. Eckstein J. The three-dimensional substrate of atrial fibrillation in the goat. Maastricht, 2012.
14. Gharaviri A, Verheule S, Eckstein J, Potse M, Kuijpers NH, Schotten U. A computer model of endo-epicardial electrical dissociation and transmural conduction during atrial fibrillation. Europace : European pacing, arrhythmias, and cardiac electrophysiology : journal of the working groups on cardiac pacing, arrhythmias, and cardiac cellular electrophysiology of the European Society of Cardiology 2012;14 Suppl 5:v10-v16.
15. Verheule S, Tuyls E, Gharaviri A et al. Loss of continuity in the thin epicardial layer because of endomysial fibrosis increases the complexity of atrial fibrillatory conduction. Circulation Arrhythmia and electrophysiology 2013;6:202-11.
16. Verheule S, Eckstein J, Linz D et al. Role of endo-epicardial dissociation of electrical activity and transmural conduction in the development of persistent atrial fibrillation. Progress in biophysics and molecular biology 2014;115:173-85.
17. Courtemanche M, Ramirez RJ, Nattel S. Ionic mechanisms underlying human atrial action potential properties: insights from a mathematical model. The American journal of physiology 1998;275:H301-21.
18. Schotten U, Verheule S, Kirchhof P, Goette A. Pathophysiological mechanisms of atrial fibrillation: a translational appraisal. Physiological reviews 2011;91:265-325.

19. Gharaviri A, Verheule S, Eckstein J et al. How disruption of endo-epicardial electrical connections enhances endo-epicardial conduction during atrial fibrillation. Europace 2016.
20. Eijsbouts S, Ausma J, Blaauw Y, Schotten U, Duytschaever M, Allessie MA. Serial cardioversion by class IC Drugs during 4 months of persistent atrial fibrillation in the goat. J Cardiovasc Electrophysiol 2006;17:648-54.
21. Eckstein J, Verheule S, de Groot NM, Allessie M, Schotten U. Mechanisms of perpetuation of atrial fibrillation in chronically dilated atria. Progress in biophysics and molecular biology 2008;97:435-51.
22. Danse PW, Garratt CJ, Allessie MA. Flecainide widens the excitable gap at pivot points of premature turning wavefronts in rabbit ventricular myocardium. Journal of cardiovascular electrophysiology 2001;12:1010-7.
23. Danse PW, Garratt CJ, Mast F, Allessie MA. Preferential depression of conduction around a pivot point in rabbit ventricular myocardium by potassium and flecainide. Journal of cardiovascular electrophysiology 2000;11:262-73.
24. Wijffels MC, Kirchhof CJ, Dorland R, Allessie MA. Atrial fibrillation begets atrial fibrillation. A study in awake chronically instrumented goats. Circulation 1995;92:1954-68.

Figure Legends

Figure1. Dual layer model of the atrial wall (A) Model structure with two layers (epi- and endocardium) and transmural connections (grey cylinders). (B) Dissociation of electrical activity between the two layers and transmural conduction resulting in a breakthrough wave (black arrow). (C) Simulation protocol (see methods section for details). D) Number of waves per second for a control and Na^+-channel blockade simulation with 12 connections. The first 1s represent step 1 of the simulation protocol. Time points between 2s to 7s represent the step 2 of the simulation protocol. Time points between 7s to13s represent the step 3 and 4 of the simulation protocol.

Figure 2. Colour-coded membrane potentials of representative simulations with two different numbers of endo-epicardial electrical connections (conn.). A and C) Simulations without Na^+-channel blocker. B and D) Simulations with Na^+-channel blocker. The epicardial layer is shown in the top, the endocardial in the bottom panel. Snapshots are shown for every second of a simulation.

Figure3. AF persistence. Kaplan-Meier curves showing atrial fibrillation persistence with and without Na channel blockade (solid line = control, dashed line = Na^+-channel blockade) in different sets of simulations with 6, 12, 24, 48, 96 connections, and 100% connectivity (n = 8 for all different sets of simulations). Star shows significant difference between control and Na^+-channel blockade groups for different number of connections, $p<0.05$.

Figure 4. Electrophysiological parameters calculated in simulations with (blue) and without Na^+-channel blockade (black). A) AF cycle length. B) Excitable gap. C) Number of waves. D) Number of phase singularities. E) electrical activity dyssynchrony between two layers. F) Breakthrough rate per ms.

Figure5. AF persistence. Kaplan-Meier curve showing atrial fibrillation persistence with and without Na channel blockade (solid line = control, dashed line = Na^+-channel blockade) in simulations entitled in 2D and 3D group (n = 16 for all different sets of simulations). Star shows significant difference between control and Na^+-channel blockade groups for 2D simulations, $p<0.05$.

Figure 6. Measured electrophysiological parameters in slight structurally remodeled (2D) and severe structurally remodeled (3D) atrial models in control and in the presence of Na-channel block (Na-Block). A) AFCL. B) EG. C) Number of PSs. D) Number of waves. E) Breakthrough rate.

Figure 7. Examples of A) a successful BT and B) an unsuccessful BT (red circle). C) The number of unsuccessful BTs in both control and Na-blockade group.

Figure 1

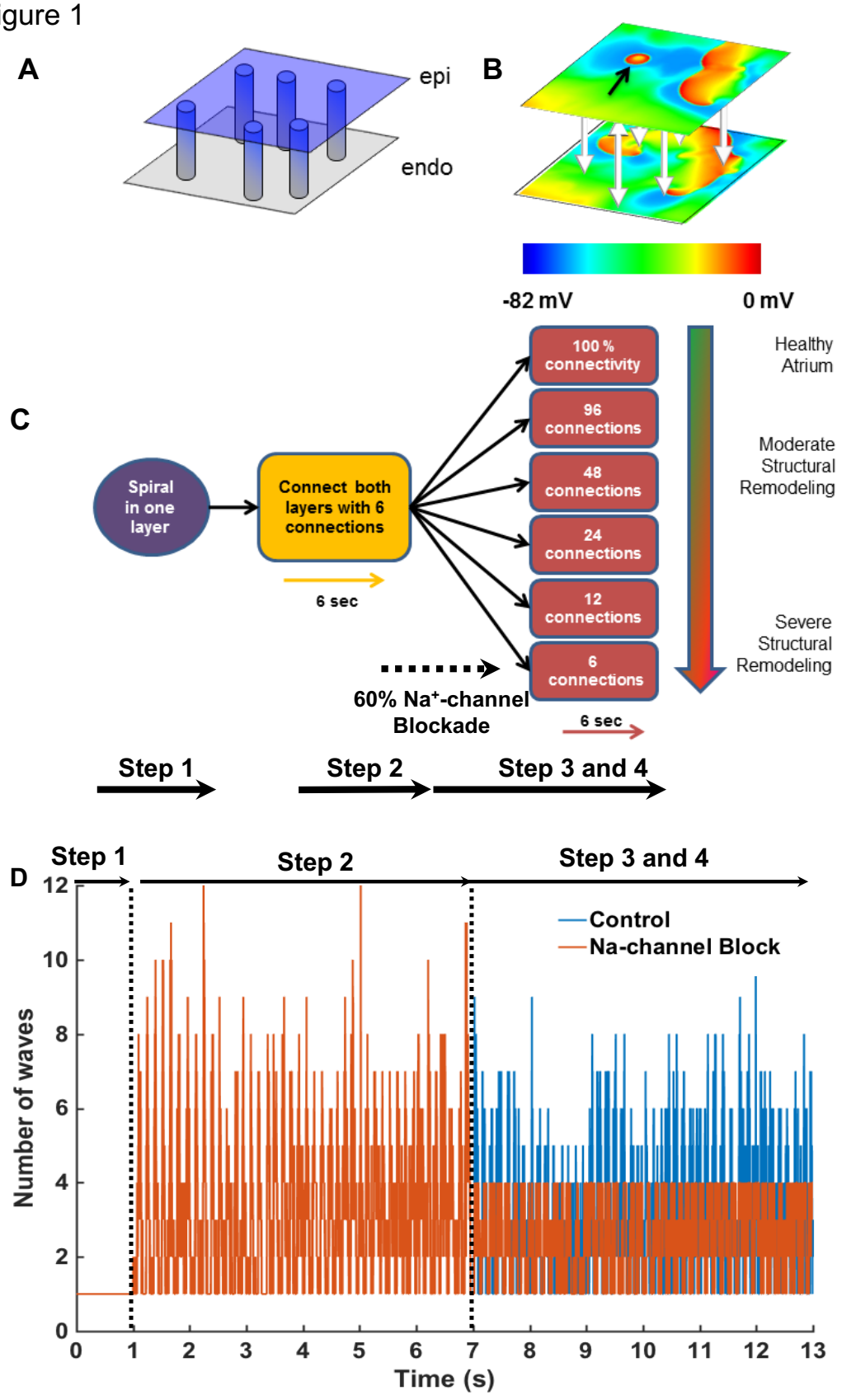
A
epi
endo
B
-82 mV
0 mV
C
Spiral in one layer
Connect both layers with 6 connections
6 sec
100 % connectivity
96 connections
48 connections
24 connections
12 connections
6 connections
Healthy Atrium
Moderate Structural Remodeling
Severe Structural Remodeling
60% Na+-channel Blockade
6 sec
Step 1
Step 2
Step 3 and 4
D
Step 1
Step 2
Step 3 and 4
Control
Na-channel Block
Number of waves
Time (s)

Figure 2

Time / N Conn.	1000 ms	2000 ms	3000 ms	4000 ms	5000 ms	6000 ms
A) 96 Conn. (Control)	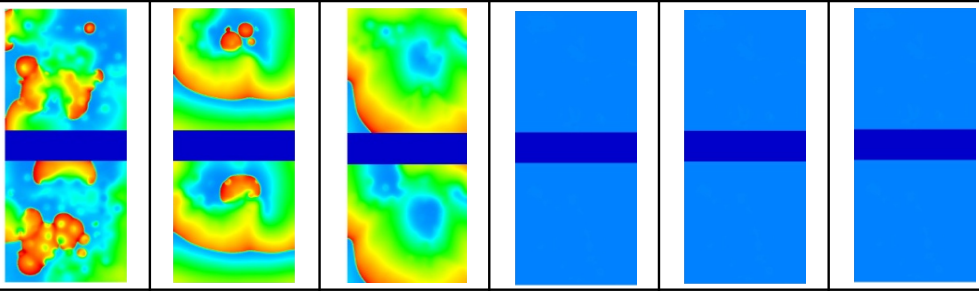					
B) 96 Conn. (Na-Block)	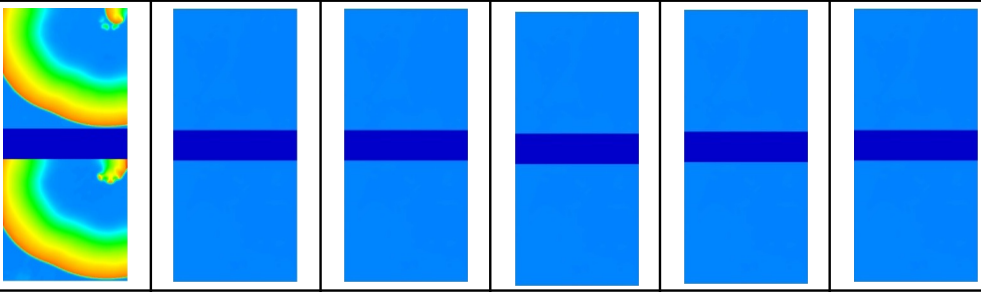					
C) 12 Conn. (control)	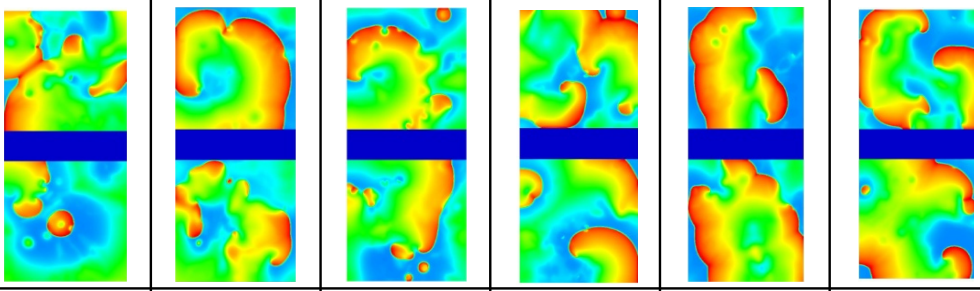					
D) 12 Conn. (Na-Block)	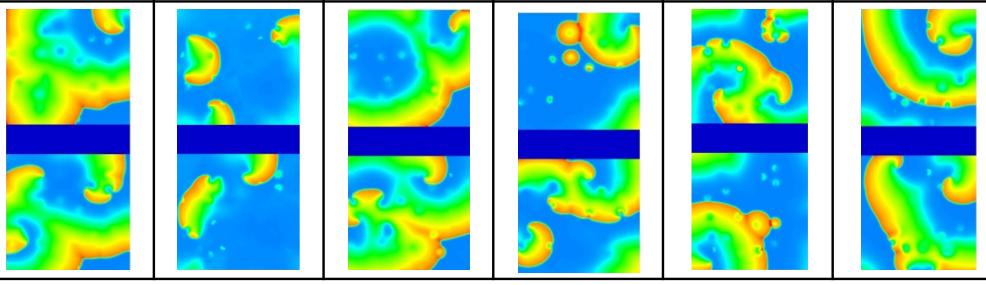					

Figure 3

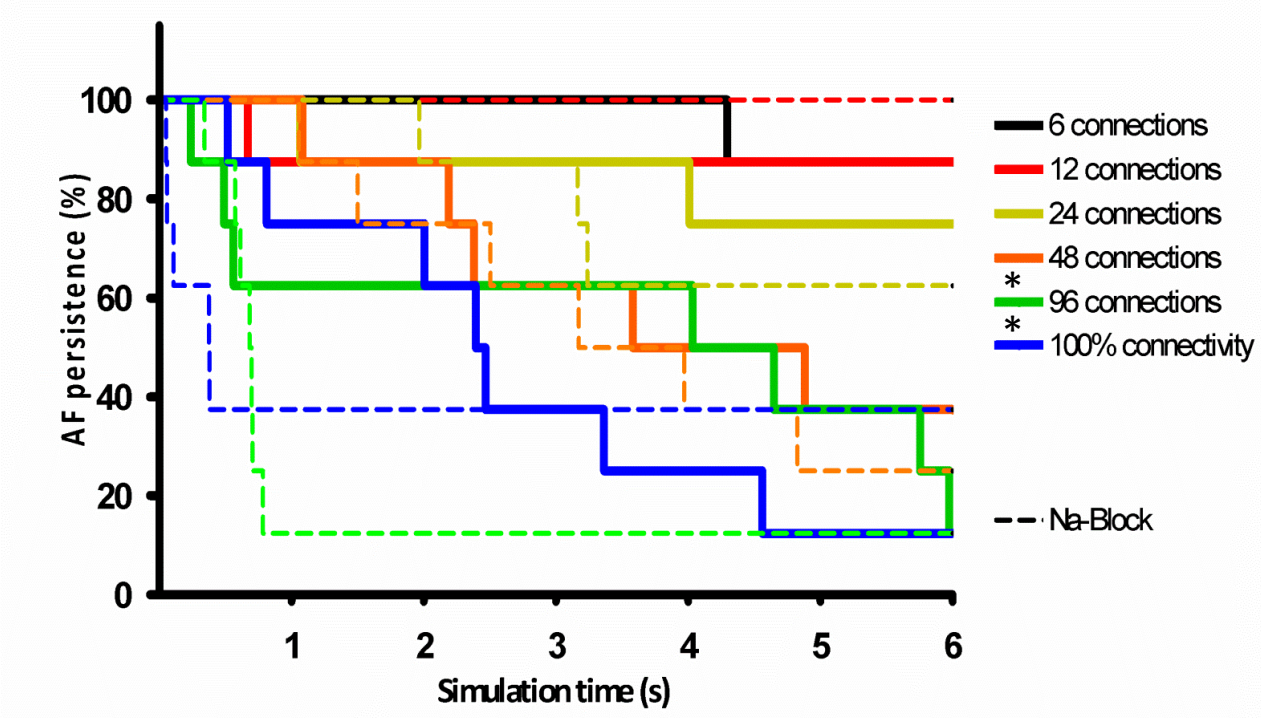
100
80
60
40
20
0
AF persistence (%)
1
2
3
4
5
6
Simulation time (s)
6 connections
12 connections
24 connections
48 connections
*
96 connections
*
100% connectivity
Na-Block

Figure 4

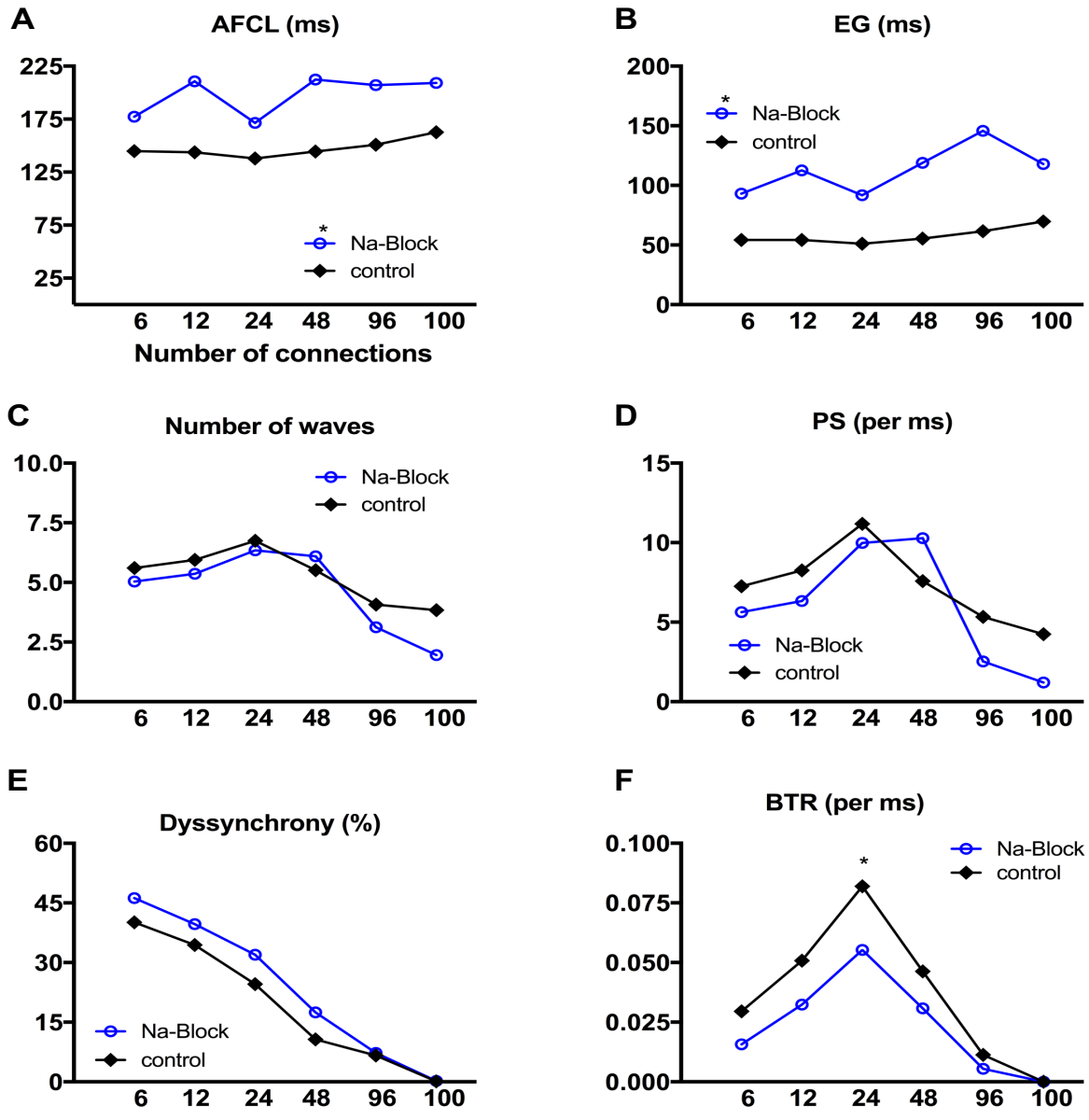
A
AFCL (ms)
225
175
125
75
25
*
Na-Block
control
6 12 24 48 96 100
Number of connections
B
EG (ms)
200
150
100
50
0
*
Na-Block
control
6 12 24 48 96 100
C
Number of waves
10.0
7.5
5.0
2.5
0.0
Na-Block
control
6 12 24 48 96 100
D
PS (per ms)
15
10
5
0
Na-Block
control
6 12 24 48 96 100
E
Dyssynchrony (%)
60
45
30
15
0
Na-Block
control
6 12 24 48 96 100
F
BTR (per ms)
0.100
0.075
0.050
0.025
0.000
*
Na-Block
control
6 12 24 48 96 100

Figure 5

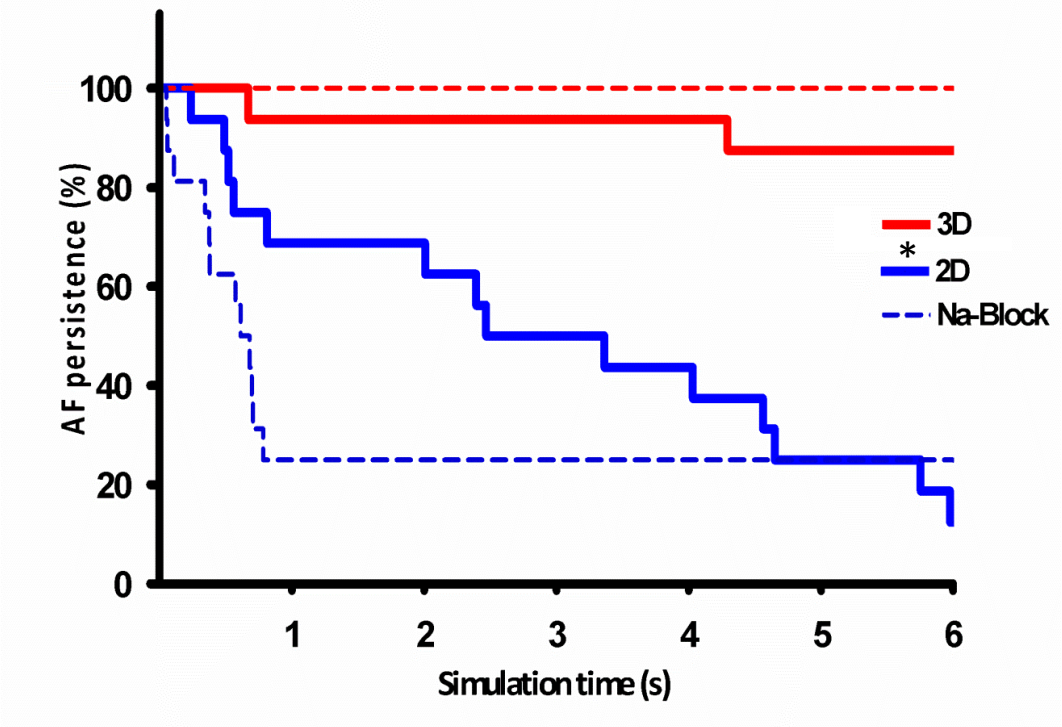
100
80
60
40
20
0
AF persistence (%)
1
2
3
4
5
6
Simulation time (s)
3D
*
2D
Na-Block

Figure 6

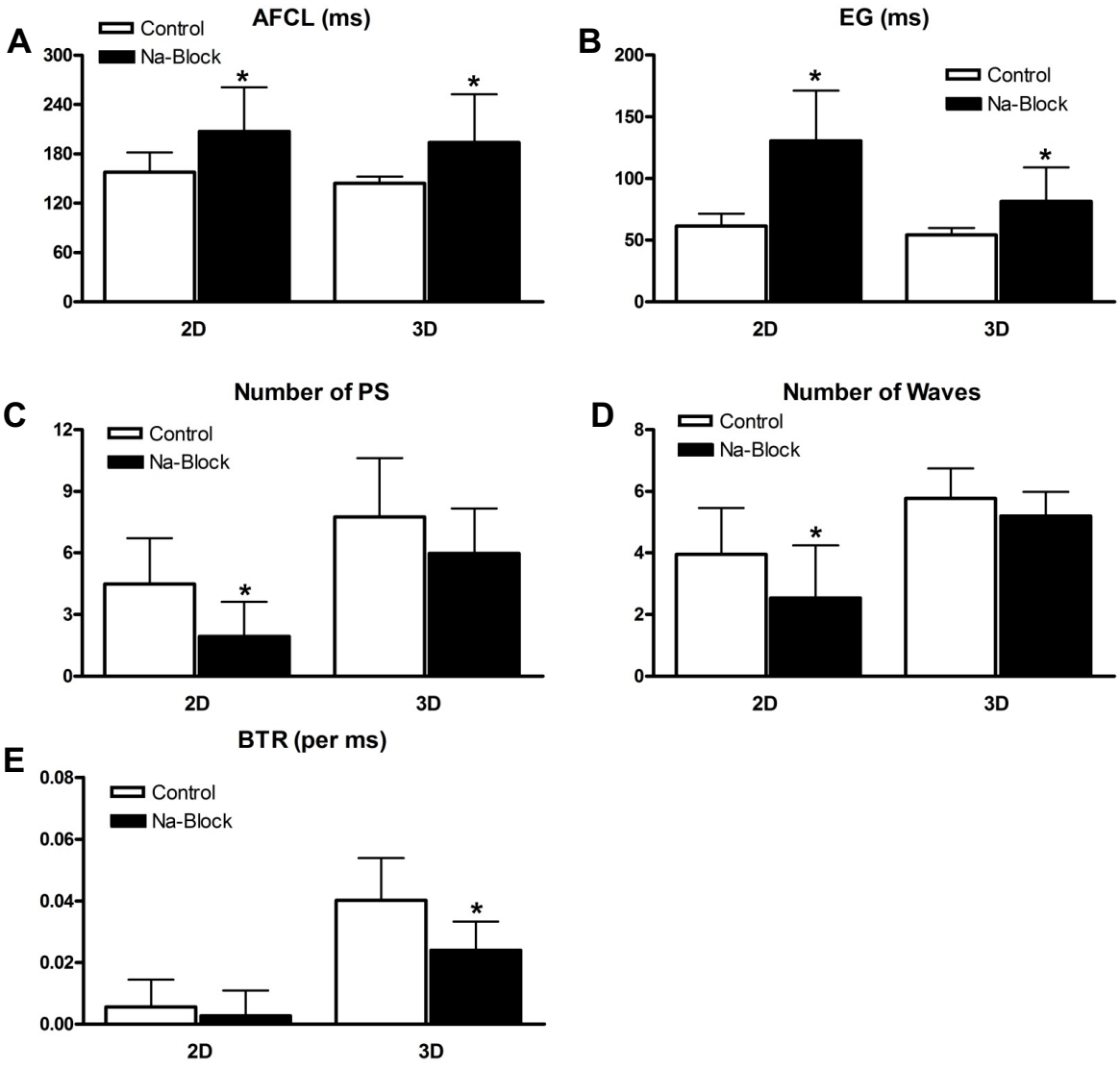
A
AFCL (ms)
Control
Na-Block
300
240
180
120
60
0
2D
3D
B
EG (ms)
200
150
100
50
0
C
Number of PS
12
9
6
3
0
D
Number of Waves
8
6
4
2
0
E
BTR (per ms)
0.08
0.06
0.04
0.02
0.00

Figure 7

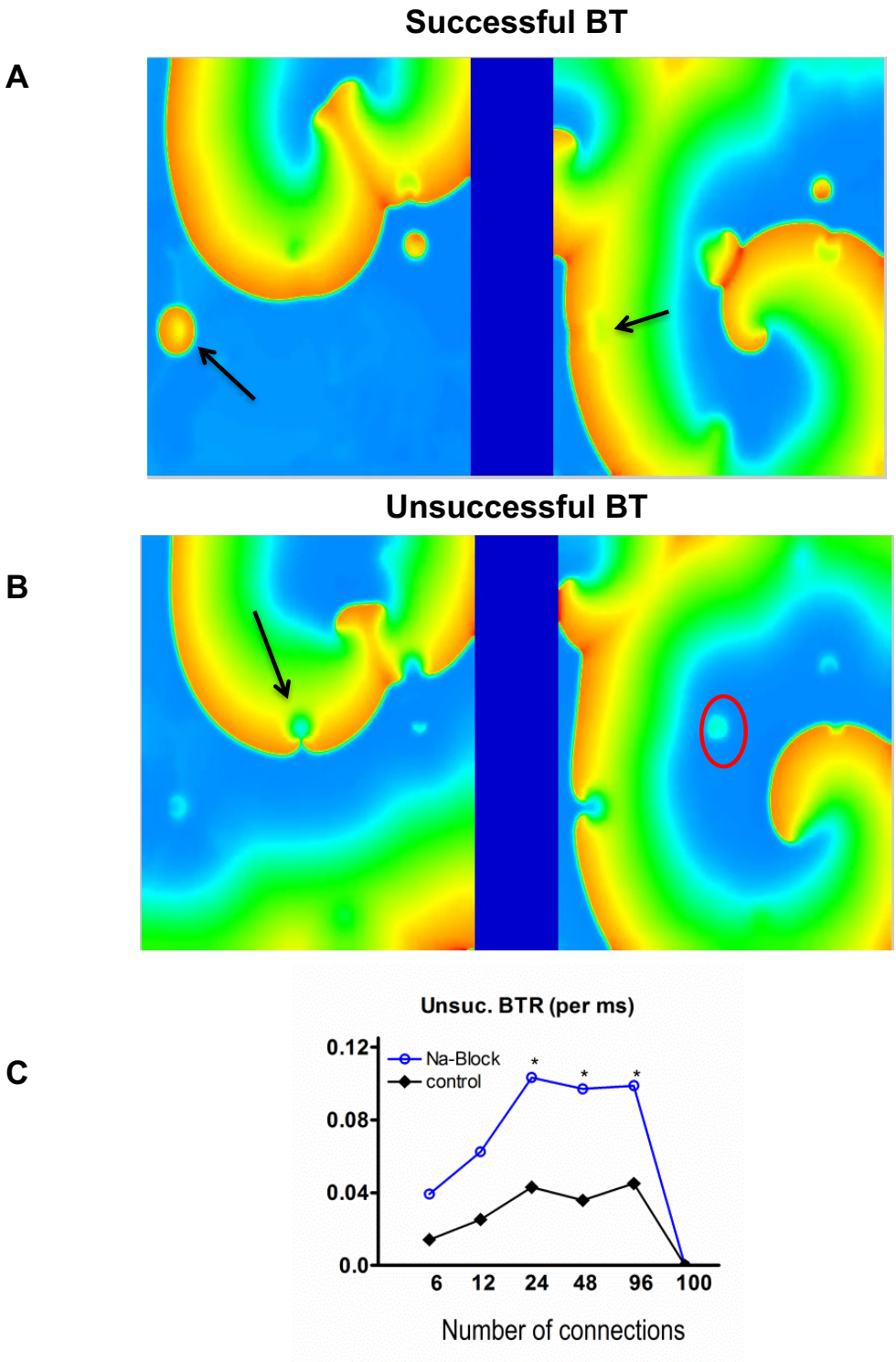
Successful BT
A
Unsuccessful BT
B
C
Unsuc. BTR (per ms)
0.12
0.08
0.04
0.0
Na-Block
control
*
*
*
6
12
24
48
96
100
Number of connections